A Deep Adversarial Model for Segmentation Assisted COVID-19 Diagnosis Using CT Images

Hai-yan Yao (yaohywqh@shu.edu.cn)
Shanghai University https://orcid.org/0000-0002-5706-9215
Wang-gen Wan
Shanghai University
Xiang Li
Shanghai University

Research Article

Keywords: deep adversarial model, CT image, COVID-19, deep learning

Posted Date: December 13th, 2021

DOI: https://doi.org/10.21203/rs.3.rs-1147701/v1

Version of Record: A version of this preprint was published at EURASIP Journal on Advances in Signal Processing on February 10th, 2022. See the published version at https://doi.org/10.1186/s13634-022-00842-x.

RESEARCH

A deep adversarial model for segmentation assisted COVID-19 diagnosis using CT images

Hai-yan Yao[1,2*], Wang-gen Wan[1] and Xiang Li[1]

*Correspondence:
yaohywqh@shu.edu.cn
[1]School of Communication and Information Engineering, Shanghai University, Shanghai, China
Full list of author information is available at the end of the article

Abstract

The outbreak of coronavirus disease 2019(COVID-19) is spreading rapidly around the world, resulting in a global pandemic. Imaging techniques such as computed tomography (CT) play an essential role in the diagnosis and treatment of the disease since lung infection or pneumonia is a common complication. However, training a deep network to learn how to diagnose COVID-19 rapidly and accurately in CT images and segment the infected regions like a radiologist is challenging. Since the infectious area are difficult to distinguish, and manually annotation the segmentation results is time-consuming. To tackle these problems, we propose an efficient method based on a deep adversarial network to segment the infection regions automatically. Then the predicted segment results can assist the diagnosis network in identifying the COVID-19 samples from the CT images. On the other hand, a radiologist-like segmentation network provides detailed information of the infectious regions by separating areas of ground-glass, consolidation, and pleural effusion, respectively. Our method can accurately predict the COVID-19 infectious probability and provides lesion regions in CT images with limited training data. Additionally, we have established a public dataset for multitask learning. Extensive experiments on diagnoses and segmentation show superior performance over state-of-the-art methods.

Keywords: deep adversarial model; CT image; COVID-19; deep learning

1 Introduction

The outbreak of coronavirus disease 2019(COVID-19) is spreading rapidly around the world, resulting in a global pandemic. Timely and accurate detection of the disease is crucial, which would enable the implementation of all the supportive care required by patients affected by COVD-19. Infected patients with pneumonia may present on medical imaging, such as chest X-ray (CXR) and computed tomography (CT) images. Compared to X-rays, CT screening is widely preferred due to its merit, and it already plays a significant role in confirming positive COVID-19 patients. A quick and accurate diagnosis and infection annotation by a radiologist is needed, since the current high-quality pixel-level annotation of lung infections in CT slices is expensive and time-consuming.

Training a deep network to learn how to diagnose COVID-19 rapidly and accurately in CT images is challenging because the infectious areas are difficult to distinguish. To address these problems, some deep learning based methods were proposed and utilized in infection detection [1, 2, 3, 4], segmentation infection regions [5], classification [6, 7, 8], diagnosis [9, 10, 11] of COVID-19. Some semi-supervised framework [12, 13] have demonstrated good performance due to its high capability

of feature extraction. The segmentation methods in COVID-19 application can be mainly grouped into lung regions [14, 15, 8], and lung-lesion regions [5, 16],In terms of the target region of interest (RoI). Since the lesions or nodules could be small with a variety of shapes and textures, locating them is a challenging task. But it is important for further diagnosis.

However, almost all of these methods diagnose by feeding the entire CT image or pre-processing patches of the region of interest (RoI). There could be two limitations to this strategy. Firstly, only the classification results are given without a proper inference process makes the judgment credibility decline. We aim to provide a clinical diagnosis ahead of the pathogenic test to save critical time for disease control. Secondly, the deep model based on the original CT images cannot make full use of the graphical features, leading to false positive and false negative in the data. Thus, we argue that handling this problem using segmentation of the abnormal areas, such as ground-glass, consolidation and pleural effusion, aiming to assist the classification could be more convincing and effective. Concerned with the COVID-19 radio-graphical changes in CT images, we aim to develop a model that could not only predict COVID-19's segmentation of the abnormality but also provide a clinical diagnosis ahead of the pathogenic test, thus saving critical time for disease control.

Inspired by the successful utilization of generative adversarial networks (GANs) in images to videos, we propose a deep adversarial model. Since a standard GAN model [17] is proposed, they have been shown to generate compelling results in a wide variety of applications. Specifically, in the field of medical image segmentation, various GAN-based methods [18, 19, 20, 21, 22]have been proposed recently. We try to assist the diagnosis by the accurate segmentation of the infection areas generated by GANs. Moreover, to address the problem of data shortage in the early stage, we try to adopt knowledge distillation[23, 24, 25, 26] from unbalanced samples.

In summary, we propose a quick and efficient solution to overcome the above issues. Firstly, we employ a GAN to segment the infection areas from the CT image automatically. It is helpful to alleviate the health services by providing a faster way of objectively evaluating the radiological CT images. Efficient segmentation is the key point in further clinical diagnosis. Secondly, in order to separate the COVID-19 from other diseases, the corresponding annotation can give powerful assistance. The reason is that image segmentation is also a marking process, which implies semantic information and detailed features. Therefore we construct a deep adversarial network that can predict COVID-19's segmentation of the abnormality, and provide a clinical diagnosis ahead of the pathogenic test, thus saving critical time for disease control.

2 Materials and methods

2.1 Datasets

As we can see in Table 1, existing public datasets are either for diagnosis or for segmentation tasks. The COVID-19 CT segmentation dataset [27] is the first one for segmentation, contains 100 axial CT images from 60 patients with COVID-19. Each image is segmented by a radiologist using 3 labels: ground-glass (mask value = 1), consolidation (mask value = 2) and pleural effusion (mask value = 3). Then,

COVID-SemiSeg[12] dataset adds 1600 unlabeled images from the COVID-19 CT Collection dataset[28] for augmenting the training data. It is helpful for training a deep network to diagnose like a radiologist. Inspired by it, we collect a COVID-19 radiologist dataset for multitask learning. For the segmentation task, we employ our network on the 100 images with segment labels from COVID-19 CT segmentation dataset [27]. The images are resized, grey-scaled, and compiled into a single NIFTI-file (512 x 512 x 110). We split the 100 images into 5 equal folds, using 4 of them for training, and 1 for testing. Then we iterate over which fold is the test set, evaluate the performance, and finally average the performance across the different folds. For the diagnosis task, the training set consists of 100 COVID images used in the segmentation task and another 100 non-COVID images from COVID-CT-Dataset [29]. Further, we collect another 275 COVID images and 818 non-COVID images for testing. In this way, we implement our deep adversarial network and verify that the segmentation results can improve the diagnosis performance. The experimental results demonstrate the effectiveness of the proposed approach.

For the diagnosis task, the performance of the model was evaluated by assessing the classification accuracy, precision, recall, and F1 scores. The accuracy of a method determines how correct the values are predicted. The precision determines the reproducibility of the measurement or how many of the predictions are correct. Recall shows how many of the correct results are discovered. F1 score uses a combination of precision and recalls to calculate a balanced average result. For the segmentation task, we evaluate the results by pixel accuracy (PA). It is the simplest metric defined as the ratio of the marking correct pixels to the total pixels.

2.2 Semantic segmentation network

At the very beginning, we think of using a classifier to directly diagnose whether the sample is from COVID-19 positive patients or not. VGG [34] model is selected. We feed the positive and negative samples into a pre-trained model, but the results are not satisfactory. Reasons for the low accuracy are unbalanced training data and high similarity between positive and negative samples. In clinical practice, a radiologist can recognize infection regions and advise on the diagnosis and further treatment. Inspired by this, we aim to train a network to segment like a radiologist and take the segment region as a guide to improve the diagnosis results.

In Figure 1 we provide a schematic representation of the overall framework. The input to our system is CT images waiting for diagnosing and screening. The architecture consists of two main processes: the GAN network takes the CT image as input and segments the region of the abnormal area from the background. Furthermore, the deep neural network takes the CT scan, and the corresponding predicted mask together as input, aiming to diagnose whether it is the COVID-19 or not. In this way, the semantic information can assist the pathogenic test, thus saving critical time and improving accuracy. We present the details of our framework in the following sections.

At the first step of our method, we attempt to employ a semantic segmentation network (SSN), a GAN-based network, to force the generated semantic segmentation mask to be more consistent and close to the ground truth. Given image domain X and mask domain M, the semantic segmentation aims to learn the mapping from

a CT scan to a binary mask, G_{XM}: $X \rightarrow M$, *i.e.*, segmenting target pixels around abnormality. For generator G, it aims to generate a mask that approaches the ground truth. For the discriminator D, it can be denoted as $(M, M_{GT}) \rightarrow [real/fake]$, distinguishing the true mask from the fake ones. GANs are learned by playing a minimax optimization game between a generator network G and a discriminator network D. Through this adversarial process, the GANs are capable of learning a generative distribution that matches the empirical distribution of a given data collection. Note that our target is not only generating the mask of abnormality but also aiding the further disease diagnosis. The network requires an accurate segmentation to predict both in location, area, and proportion.

We express the adversarial loss as:

$$L_A = \min_{\theta g} \max_{\theta d} \mathbb{E}_x[log(1 - D(G(x)))] + \mathbb{E}_m[logD(m)] \tag{1}$$

where x is the sample of the original CT image, and m is the relevant segmentation mask ground truth. θ_g and θ_d denote the parameters of the network layers of the G and D, respectively. We get these parameters by minimizing the loss of G net and maximizing the loss of D net.

To enhance the efficiency of the segmentation network, a segmentation loss is introduced. In the training process, the MSE loss between the generated mask $G(x)$ (the mapping result of input CT image x obtained by the generator G) and the ground truth mask M_{GT} of the infectious region. The segmentation loss is defined as following:

$$L_{seg} = MSE(G(x) - M_{GT}) \tag{2}$$

The final objective is defined as following:

$$L_{final} = L_A + \lambda L_{seg} \tag{3}$$

where λ keeps the balance of the two objectives. We set $\lambda_1 = 10$ in training.

The CT images feeding to the generator G are resized to 512×512. It consists of 24 layers (3 layers for the encoder, 18layers for the transformer, and 3layers for the decoder, respectively). In detail, nine residual blocks [35] are used in the transformer, and instance normalization [36] is utilized in the net. Additionally, the discriminator D contains 5 convolution layers. In G and D, the parameters are 11.37M and 2.76M, respectively. We summarize the proposed training procedure for our method in Algorithm 1.

2.3 Segmentation assisted COVID-19 diagnosis

We fine-tune a pre-trained classifier using VGG-16[34] architecture model to classify the COVID-19 positive patients and others. To provide the semantic information and detailed features to assist the CT slice, we concatenate the generated mask M and the original CT image as the input of the classifier, which is denoted as: $concat(X_i, M_i) \rightarrow y$, where y denotes the label [0,1]. The parameters are about

Algorithm 1: The training algorithm

Input: Dataset $D = \{x_i, y_i, m_i\}_{i=0}^{N-1}$ (image, label, mask GT)
Output: Parameters $\theta_g, \theta_d, \theta_c$
Initial Gnet, Dnet, Cnet (generator net, discrimitor net, classify net)
for *epoch = 0 → (max_iterations-1)* **do**
  for *i=0 → (N-1)* **do**
    $/\star\, m' : predict\ mask \star/$
    $m' = \mathsf{Gnet}(x_i)$;
    $d_{out} = \mathsf{Dnet}(m')$;
    xm=concatenate(x_i, m');
    $y' = \mathsf{Cnet}(xm)$;
    $L_{seg} = \mathsf{MSEloss}\ (m', m_i)$;
    $L_A = \mathsf{MSEloss}\ (d_{out}, 1)$;
    $/\star\, L_G : GnetLoss \star/$
    $L_G = L_{seg} + \lambda L_A$;
    $/\star\, L_D : DnetLoss \star/$
    $L_D = \mathsf{MSEloss}\ (d_{out}, 0) + \mathsf{MSEloss}\ (\mathsf{Dnet}(m_i), 1)$;
    $/\star\, L_C : CnetLoss \star/$
    $L_C = \mathsf{CrossEntropyloss}\ (y', y_i)$;
    Train Gnet, Dnet, Cnet and update $\theta_g, \theta_d, \theta_c$ by descending L_G, L_D, L_C
  end
end

134.27M. In the training process, the cross-entropy loss is used as the classification loss.

$$L_{cls} = CrossEntropy(G(x, m) - y) \tag{4}$$

2.4 Segment like a radiologist

Aiming to make the network work as a radiologist and correctly annotate different areas, we implement a parallel training strategy. COVID-19 CT segmentation dataset contains images segmented in 3 labels: ground-glass, consolidation, and pleural effusion with mask values 1, 2, and 3, respectively. We propose the radiologist-like segmentation network (RSN) for the segmentation and diagnosis of multi-sort CT images which is shown in Figure 2. We feed three types of mask data into SSN, accompanied by the original CT image. After parallel training, each SSN can separate different classes of the mask (ground-glass, consolidation, and pleural effusion). The segmentation results of different classes are composited into one image, then we can achieve the prediction of radiologist-like annotation on infectious areas. The powerful capability of SSN ensures the good performance of RSN, even with imbalanced training data. On chest imaging of COVID-19, multiple small patch shadows and interstitial changes are presented in the early stage, and then numerous ground-glass shadows are developed in both lungs. In severe cases, lung consolidation could occur, and pleural effusion is rare. We observed very little labeling data for the third category (pleural effusion), leading to training failures. The experimental results show good prediction in the correct position and the correct classification. This detailed, radiologist-like segmentation can give doctors great help in determining the extreme severity of the disease.

2.5 Data distillation for COVID-19 diagnosis

We propose data distillation for COVID-19 diagnosis using a deep adversarial network. To address the problem of insufficient data, we leverage data distillation on unlabeled data. Firstly, we train a teacher model on manually labeled data. Secondly, the trained model is applied for segmentation. Then we convert the predictions on the unlabeled data into labels by assembling the multiple predictions. Finally, the model is retrained on a new training set consisting of manually labeled data and automatically labeled data. The aim is to mine latent information in the data at hand, including limited labeled samples and more unlabeled samples. It is helpful to improve the performance of the network.

3 Experimental results and discussions

3.1 Segmentation results and analysis.

The segmentation results can visually see the infection areas, which is more beneficial for clinicians to diagnose the disease. So we implement the typical infection segmentation firstly. Then, aiming to show the detailed result, we train the network to segment like a radiologist.

Typical infection segmentation We feed the slices to SSN and train it to segment the infection region. In Figure 3, we can see the typical infection segmentation (TIS) results of SSN, from which we achieve high-quality segmentation masks for each pulmonary infection area. Except for the small parts on the boundary that are error-prone, as shown in the annotated section in the bottom row. This may be due to the network's inadequate identification of small and fragmented targets, but it does not affect the estimation of COVID-19. We can achieve infection segmentation and COVID-19 classification at the same time. The comparison results of different segmentation methods are shown in Table 2, we can see the proposed TIS can get higher performance.

Radiologist-like segmentation Furthermore, to make the network work as a radiologist, we train the SSN in a parallel strategy. The refined segmentation results are shown in Figure 4. The blue part, yellow part, and green part represent ground-glass, consolidation, and pleural effusion, respectively. Compared to the ground truth segmentation annotated by a real radiologist, the network can provide similar results, especially ground-glass (blue) and consolidation area (yellow).

Radiologist-like segmentation is more challenging than infection segmentation because it requires not only segmentation but also classification of the results. Therefore, it is prone to confuse when discriminating different classes of infection regions. Take the result on the right of the fourth row in Figure 4 as an example, consolidation is misjudged as ground-glass (i.e., misjudge the blue part as yellow).

Since background accounts for a large proportion in the single CT image, it leads to a high accuracy close to 1. So in statistics, only the segment target pixels are considered without background. When we train the SSN and calculate the L1loss between the real mask and the generated mask, class 1 and class 2 segment results are acceptable. But the segmented effect of class 3 is not obvious. Then, we change to use MSEloss for training, the class 3 segmentation results are improved, and the other two classes are also enhanced remarkably. The results are shown in Table 3. Also, we compare the result with Mask-RCNN, which is good at the segmentation

task. The proposed method performs better scores in many ways, except slightly lower PA scores in class 1. Compared to others, class 3 segmentation is more challenging. The reason for difficult training is the relatively limited amount of data containing a very small target size. We also use parallel strategy in this case. To increase the proportion of class 3 samples in training, we split the train set into class 3 and non-class 3 and randomly select samples in each batch. Rotation, flip, and crop are also used for data augmentation.

3.2 COVID-19 diagnosis results.

We show the effect of mask assistant prediction. We train and test our network on the COVID-19 radiologist dataset and achieve a good result. Considering that the classification does not occur simultaneously with segmentation, we select a more robust model after segmentation to assist the classification procedure (with mask). Compared with the direct classified (without mask), we can see that the estimated mask from SSN can significantly improve the classification result. In addition, the classify results with Mask-RCNN segment assistant are shown as a comparison in Table 4, which is a little bit lower than the proposed method.

3.3 Data distillation results.

Data distillation can boost the performance of segment results, as shown in Figure 5. For clarity, we exploit a comparison experiment on radiologist-like segmentation. The segmentation labels of class 1, which means ground glass, have obvious edges and can distinguish the target area and non-target area after data distillation. The reason is to Mine the information in the existing labeled data. For unlabeled data, we also make full use of the hidden information for further prediction. Yet it has limits. The data distillation has been proved capable of tackling the problem of the insufficient data problem by utilizing more unlabeled samples, but incapable of keeping the certainty in training since introducing error-prone labels, so-called pseudo labels, as ground truth.

3.4 Discussion

As our experimental results showed, we achieve promising results in COVID-19 diagnosis, and segmentation of the infection regions such as ground glass, consolidation, and pleural effusion regions. These results are helpful for clinicians to make a rapid diagnosis and treatment plans. There are two advantages to the deep adversarial model. Firstly, we conduct a cascade strategy to achieve segmentation and diagnosis. The results generated by SSN serve as the auxiliary of the original CT image, thus improving the performance of the diagnosis. Secondly, it is simple to use, and no complicated techniques are introduced. The results of diagnosis and segmentation are mutually promoted. Moreover, we can clearly see or estimate the performance of each step.

Even though there are some limitations. Firstly, when we conduct a multi-step strategy to solve a complex task, it is obvious that each step's training objective is not consistent. How to balance the relation and train the network to achieve optimal performance is a challenge because the deviation from one step may affect another. In the future, we will focus on constructing an end-to-end network to

tackle this problem. Secondly, the problem of efficient learning on an unbalanced data. Annotation data are challenging since it needs an experienced radiologist and manually labeling different kinds of pulmonary infection areas with different labels is time-consuming. Even though we use a parallel strategy, training the network to learn one class each time, the very small sample size in one category is still a challenge. We will study to optimize the model to make full use of the existing samples in the future. Moreover, we will do much more work on 3D-CNN since it performs better to determine or confirm lesions, particularly for the lung CT.

4 Conclusion

In this work, we present a conceptually effective and flexible framework for COVID-19 diagnosis and radiologist-like localization of the lung's infectious region. Our approach efficiently detects the abnormal region in the CT images while simultaneously classify the COVID-19 positive patients from others. We introduce a deep adversarial network that can generate the location of the infection region. The segmentation results bring detailed and important information to the classifier, which acts as a guide. This information effectively improves the COVID-19 diagnosis accuracy. The experiments have shown successful results on both of the tasks. Moreover, we try to tackle the problem of unbalanced data in the training process. A parallel training strategy for different classes of data achieves great improvement. Along with enhancing artificial intelligent technology, the approaches to deal with data shortage and imbalanced data will be more effective, which is bound to boost the relevant processing.

In conclusion, the purpose of our deep adversarial model is to automatically screen the infectious area in lung CT image while simultaneously diagnosing the COVID-19 positive patients from others, reducing the burden of labor and avoiding possible omissions. We will reduce the time it takes and try to put it to practical use.

Acknowledgements
This work was supported by Research Foundation of Anyang Institute of Technology [YPY2021007] and Youth Foundation of Anyang Institute of Technology [QJJ2016001].

Funding
This work was supported by Research Foundation of Anyang Institute of Technology [YPY2021007] and Youth Foundation of Anyang Institute of Technology [QJJ2016001].

Abbreviations
COVID-19: Coronavirus disease of 2019; CT: Computed tomography; CXR: Chest X-ray; RoI: Region of interest; GAN: Generative adversarial network; VGG: Visual Geometry Group; SSN: Semantic segmentation network; RSN: Radiologist-like segmentation network; TIS: Typical infection segmentation.

Availability of data and materials
All the data are available upon request from the corresponding author.

Ethics approval and consent to participate
Not applicable. All the databases were obtained from the literature that are publicly available.

Competing interests
The authors declare that they have no competing interests.

Consent for publication
Not applicable.

Authors' contributions
All the authors contributing equally in data collection, processing, experiments, and article writing. The authors read and approved the final manuscript.

Authors' information

Hai-yan Yao

She received the B.S. degree from Zhengzhou University, Zhengzhou, China, in 2004, and the M.S. degree from the Nanjing University of Science and Technology, Nanjing, China, in 2011. She is currently pursuing the Ph.D. degree with the Institute of Smart City, School of Communication and Information Engineering, Shanghai University, China. She was with the Department of Electronic Information and Electrical Engineering, Anyang Institute of Technology, China. Her current research interests include computer vision and machine learning.

Wang-gen Wan

He received the Ph.D. degree in information and signal processing from Xidian University, China, in 1992. He is currently a Professor with the School of Communication and Information Engineering, the Program Leader for Circuits and Systems, and the Dean of the Institute of Smart City, Shanghai University, China. He has been awarded funding as the principal investigator of more than 30 government research projects. He is the coauthor of approximately 200 academic articles. His research interests include VR/AR, artificial intelligence, video processing, machine learning, and data mining. He is an IET Fellow, the Chairman of IET Shanghai Local Network, and the Vice-Chairman of the IEEE Shanghai CIS Chapter. He has served as the co-chairman of at least 10 international conferences, since 2008.

Xiang Li

He received the B.S. degree from the Tianjin University of Technology and Education, Tianjin, China, in 2001, and the M.S. degree from Jiangsu University, Zhenjiang, China, in 2008. He is currently pursuing the Ph.D. degree in signal and information processing with Shanghai University, China. His current research interests include artificial intelligence and deep learning.

Author details

[1]School of Communication and Information Engineering, Shanghai University, Shanghai, China. [2] , Anyang Institute of Technology, Anyang, China.

References

1. C.Huang, Y.Wang, X.Li, L.Ren, B. Cao, Clinical features of patients infected with 2019 novel coronavirus in Wuhan, China. *Lancet,* **395** 497–506 (2020).
2. M. Z.Alom, M.Rahman, M. S.Nasrin, T. M.Taha, V. K.Asari, COVID MTNet: COVID-19 detection with multi-task deep learning approaches. *arXiv* , arXiv:2004.03747 (2020).
3. V.Rajinikanth, N.Dey, A.Raj, A. E.Hassanien, K. C.Santosh, M.Sri Harmony-search and otsu based system for coronavirus disease (COVID-19) detection using lung CT scan images.*arXiv* arXiv:2004.03431 (2020).
4. K.Hammoudi, H.Benhabiles, M.Melkemi, F.Dornaika, A.Scherpereel, Deep learning on chest X-ray images to detect and evaluate pneumonia cases at the era of COVID-19. *Journal of Medical Syestems* **45** (2021).
5. F.Shan, Y.Gao, J.Wang, W.Shi, N.Shi, M.Han, Abnormal lung quantification in chest CT images of COVID-19 patients with deep learning and its application to severity prediction.*Medical Physics* **48** 1633-1645 (2021).
6. L.Li, L.Qin, Z.Xu, Y.Yin, X.Wang, B.Kong, Artificial intelligence distinguishes COVID-19 from community acquired pneumonia on chest CT. *Radiology* pp. 200905 (2020).
7. S.Wang, B.Kang, J.Ma, X.Zeng, B.Xu, A deep learning algorithm using CT images to screen for Corona Virus Disease (COVID-19). *European Radiology* (2021).
8. O.Gozes, M.Frid-Adar, H.Greenspan, P. D.Browning, H.Zhang, W.Ji, A.Bernheim, E. Siegel, Rapid AI Development Cycle for the Coronavirus (COVID-19)Pandemic: Initial Results for Automated Detection and Patient Monitoring using Deep Learning CT Image Analysis. *arXiv* arXiv:2003.05037v1 (2020).
9. H.Kang, L.Xia, F.Yan, Z.Wan, F.Shi, H.Yuan, H.Jiang, D.Wu, H.Sui, Sui, C.Zhang, D. Shen, Diagnosis of Coronavirus Disease 2019 (COVID-19) with Structured Latent Multi-View Representation Learning. *IEEE Transactions on Medical Imaging* **39**, 2606-2614 (2020).
10. X.Mei, H. C.Lee, K. Y.Diao, M.Huang, Y.Yang, Artificial intelligence–enabled rapid diagnosis of patients with COVID-19. *Nature Medicine* **26**, 1224 (2020).
11. Z.Wang, Q.Liu, Q.Dou, Contrastive cross-site learning with redesigned net for COVID-19 CT classification. *IEEE Journal of Biomedical and Health Informatics* **24**, 2806-2813 (2020).
12. D. P.Fan, T.Zhou, G. P.Ji, Y.Zhou, L.Shao, Inf-Net: automatic COVID-19 lung infection segmentation from CT images. *IEEE Transactions on Medical Imaging* **39**, 2626-2637(2020).
13. X.Wang, X.Deng, Q.Fu, Q.Zhou, C.Zheng, A weakly-supervised framework for COVID-19 classification and lesion localization from chest CT. *IEEE Transactions on Medical Imaging* **39**, 2615-2625(2020).
14. C.Zheng, X.Deng, Q.Fu, Q.Zhou, X.Wang, Deep learning-based detection for COVID-19 from chest CT using weak label. *medRxiv* (2020).
15. Y.Cao, Z.Xu, J.Feng, C.Jin, H.Shi, Longitudinal assessment of COVID-19 using a deep learning–based quantitative CT pipeline: Illustration of two cases. *Radiology: Cardiothoracic Imaging* **2**, e200082 (2020).
16. L.Tang, X.Zhang, Y.Wang, X.Zeng, Severe COVID-19 pneumonia: assessing inflammation burden with Volume-rendered Chest CT. *Radiology: Cardiothoracic Imaging* **2**, e200044 (2020).
17. I. J.Goodfellow, J.Pouget-Abadie, M.Mirza, X.Bing, Y.Bengio, Generative adversarial nets.*Communications of The ACM* **63**, 139-144 (2020).
18. S.Kohl, D.Bonekamp, H. P.Schlemmer, K.Yaqubi, M.Hohenfellner, B.Hadaschik, Adversarial networks for the detection of aggressive prostate cancer.*arXiv* arXiv:1702.08014 (2020).
19. S.Izadi, Z.Mirikharaji, J.Kawahara, G.Hamarneh, Generative adversarial networks to segment skin lesions. *IEEE International Symposium on Biomedical Imaging (IEEE ISBI 2018)*, pp. 881-884.
20. Z.Le, M.Pereanez, S. K.Piechnik, S.Neubauer, A. F.Frangi, Multi-input and dataset-invariant adversarial learning (MDAL) for left and right-ventricular coverage estimation in cardiac MRI. *International Conference on Medical Image Computing and Computer-Assisted Intervention MICCAI 2018*, pp. 481-489.

21. M.Rezaei, H.Yang, C.Meinel, Conditional generative refinement adversarial networks for unbalanced medical image semantic segmentation. *19th IEEE Winter Conference on Applications of Computer Vision (WACV)* , pp.1836-1845 (2019).
22. J.Tan, L.Jing, Y.Huo, Y.Tian, O.Akin, LGAN: Lung segmentation in CT scans using generative adversarial network. *Computerized Medial Imaging and Graphics* **87** (2021).
23. G.Hinton, O.Vinyals, J.Dean, Distilling the knowledge in a neural network. *NeurIPS Workshop* (2015).
24. A.Aguinaldo, P. Y.Chiang, A.Gain, A.Patil, KPearson, S.Feizi, Compressing gans using knowledge distillation. *arXiv* arXiv:1902.00159 (2019).
25. J.Yim, D.Joo, J.Bae, J.Kim, A gift from knowledge distillation: Fast optimization, network minimization and transfer learning. In Proceedings of the IEEE Conference on Computer Vision and Pattern Recognition, Honolulu, HI, USA,21–26 July 2017, pp. 7130-7138.
26. T.Li, J.Li, Z.Liu, C.& Zhang, Knowledge distillation from few samples. *arXiv* arXiv:1812.01839 (2018).
27. H.Jenssen, COVID-19 CT segmentation dataset. Available online:http://medicalsegmentation.com/covid19/.
28. Cohen,J., Morrison,P. & Dao,L. COVID-19 image data collection. *arXiv* arXiv:2003.11597 (2020).
29. J.Zhao,X.He, X.Yang, Y.Zhang, S.Zhang, P.Xie, COVID-CT-dataset: A CT scan dataset about COVID-19. *arXiv* arXiv:2003.13865 (2020).
30. COVID-19 Patients Lungs X Ray Images 10000. ,Available online: https://www.kaggle.com/nabeelsajid917/covid-19-x-ray-10000-images (2020).
31. M.Chowdhury, T.Rahman, A.Khandakar, R.Mazhar, M. A.Kadir, Z. B.Mahbub, Can AI help in screening viral and COVID-19 pneumonia?. *arXiv* arXiv:2003.13145 (2020).
32. E.Soares, P.Angelov, S.Biaso, M.Froes, D.Abe, SARS-CoV-2 CT-scan dataset: A large dataset of real patients CT scans for SARS-CoV-2 identification. *medRxiv*. Available online:https://doi.org/10.1101/2020.04.24.20078584 (2020).
33. J.Ma, G.Cheng, Y.Wang, X.An, J.Gao, Z.Yu, COVID-19 CT Lung and Infection Segmentation Dataset. *Zenodo*, Available online:doi:http://doi.org/10.5281/zenodo.3757476 (2020).
34. K.Simonyan, A.Zisserman, Very deep convolutional networks for large-scale image recognition. *Computer Science* (2014).
35. K.He, X.Zhang, S.Ren, J.Sun, Deep residual learning for image recognition. In Proceedings of the IEEE Conference on Computer Vision and Pattern Recognition, Las Vegas, NV, USA, 27-30 June 2016, pp.770–778.
36. D.Ulyanov, A.Vedaldi, V.Lempitsky, Instance normalization: The missing ingredient for fast stylization. *arXiv* arXiv:1607.08022 (2016).

Figures

Figure 1 Schematic representation of the deep adversarial network structure to screen for COVID-19 in CT image.

Figure 2 The radiologist-like segmentation network (RSN) has three SSN, which segment different areas (ground-glass, consolidation and pleural effusion), respectively.

Figure 3 Typical infection segmentation results of CT scans of COVID-19. Columns 1-3: CT image, CT image overlaid with segmentation, and ground truth, respectively.

Tables

Figure 4 Radiologist-like segmentation results of CT scans of COVID-19. Columns 1-3: CT image, CT image overlaid with segmentation, and ground truth. The blue, yellow, and green labels indicate the ground-glass, consolidation, and pleural effusion, respectively.

Figure 5 Results comparison of segmentation on CT scans. Columns 1-4: CT images, segmentation results before data distillation, segmentation results after data distillation, and ground truth, respectively.

Table 1 Comparison of the open source dataset sources of COVID-19 imaging. (Diag means diagnosis and Seg means segmentation)

Dataset	Data type	Size (Cov/NonCov)	Task-Diag	Task-Seg
COVID-19 X-ray Collection [28]	X-rays	229	✓	-
COVID-19 CT Collection [28]	CT volume	20	✓	-
COVID-CT-Dataset[29]	CT image	349/1000	✓	-
COVID-19 Patients Lungs[30]	X-rays	70/28	✓	-
COVID-19 Radiography[31]	X-rays	1143/1314/1345 (viral pneumonia)	✓	-
SARS-CoV-2 CT-scan[32]	CT image	1252/1230	✓	-
COVID-19 CT Segmentation[27]	CT image	110/0	-	✓
COVID-SemiSeg[12]	CT image	1700/0	-	✓
COVID-19 CT Lung and Infection Segmentation[33]	CT image	20/0	-	✓
COVID-19 Radiologist dataset	CT image	100/93	✓	✓

Table 2 Typical infection segmentation results comparison of different methods on covid-19 radiologist dataset.

Method	PA	IOU
Mask-RCNN	84.96%	44.8%
TIS	**85.05%**	**58.08%**

Table 3 Radiologist-like segmentation results comparison of different methods on covid-19 radiologist dataset.

Method	Class	PA	IOU
Mask-RCNN	1	**77.08%**	31.42%
L1loss	1	66.43%	46.93%
MSEloss	1	76.02%	**44.15%**
Mask-RCNN	2	46.74%	24.66%
L1loss	2	42.42%	26.82%
MSEloss	2	**62.82%**	**32.10%**
Mask-RCNN	3	26.35%	13.62%
L1loss	3	2.33%	0.27%
MSEloss	3	**30.48%**	**18.12%**

Table 4 Result comparison of different classify methods on covid-19 radiologist dataset: classifier with mask, only use classifier without SSN (W/O mask), and with SSN assistant classification (proposed), respectively.

Method	Accuracy	Precision	Recall	F1
With mask	96.04%	90.88%	94.12%	93.5%
W/O mask	95.06%	87.97%	93.09%	90.46%
Proposed	**99.2%**	**98%**	**96.0%**	**97.96%**

Figures

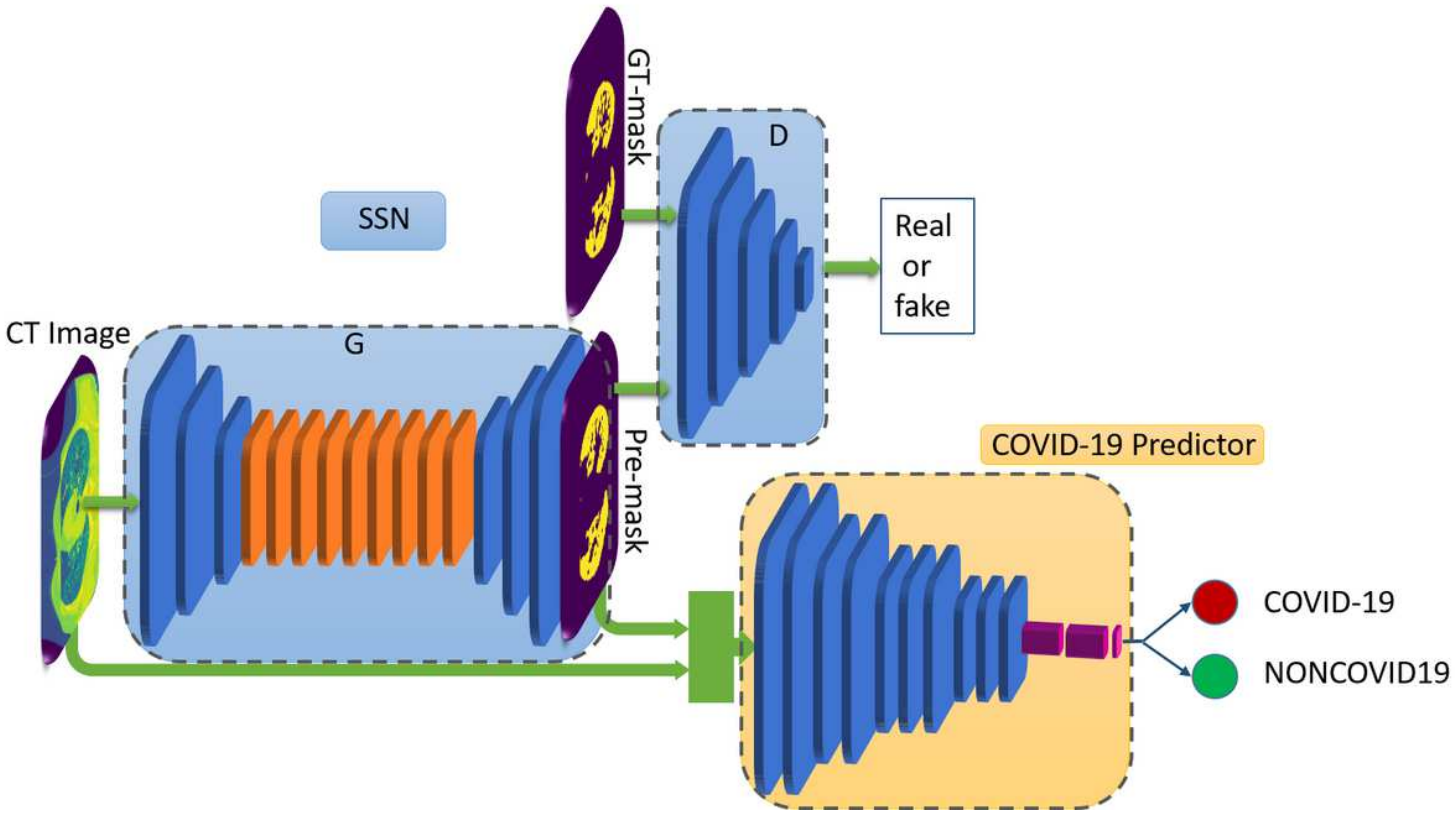

Figure 1

Schematic representation of the deep adversarial network structure to screen for COVID-19 in CT image.

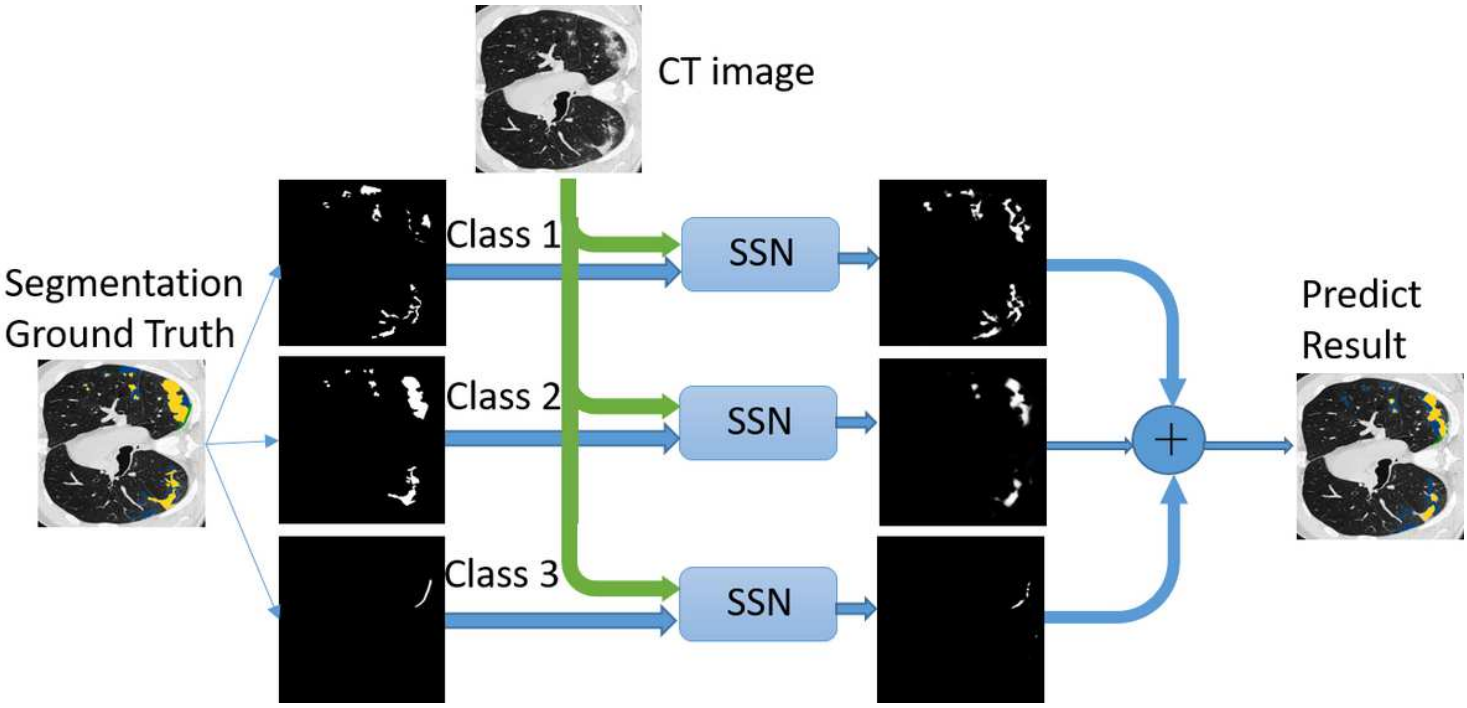

Figure 2

The radiologist-like segmentation network (RSN) has three SSN, which segment different areas (ground-glass, consolidation and pleural effusion), respectively.

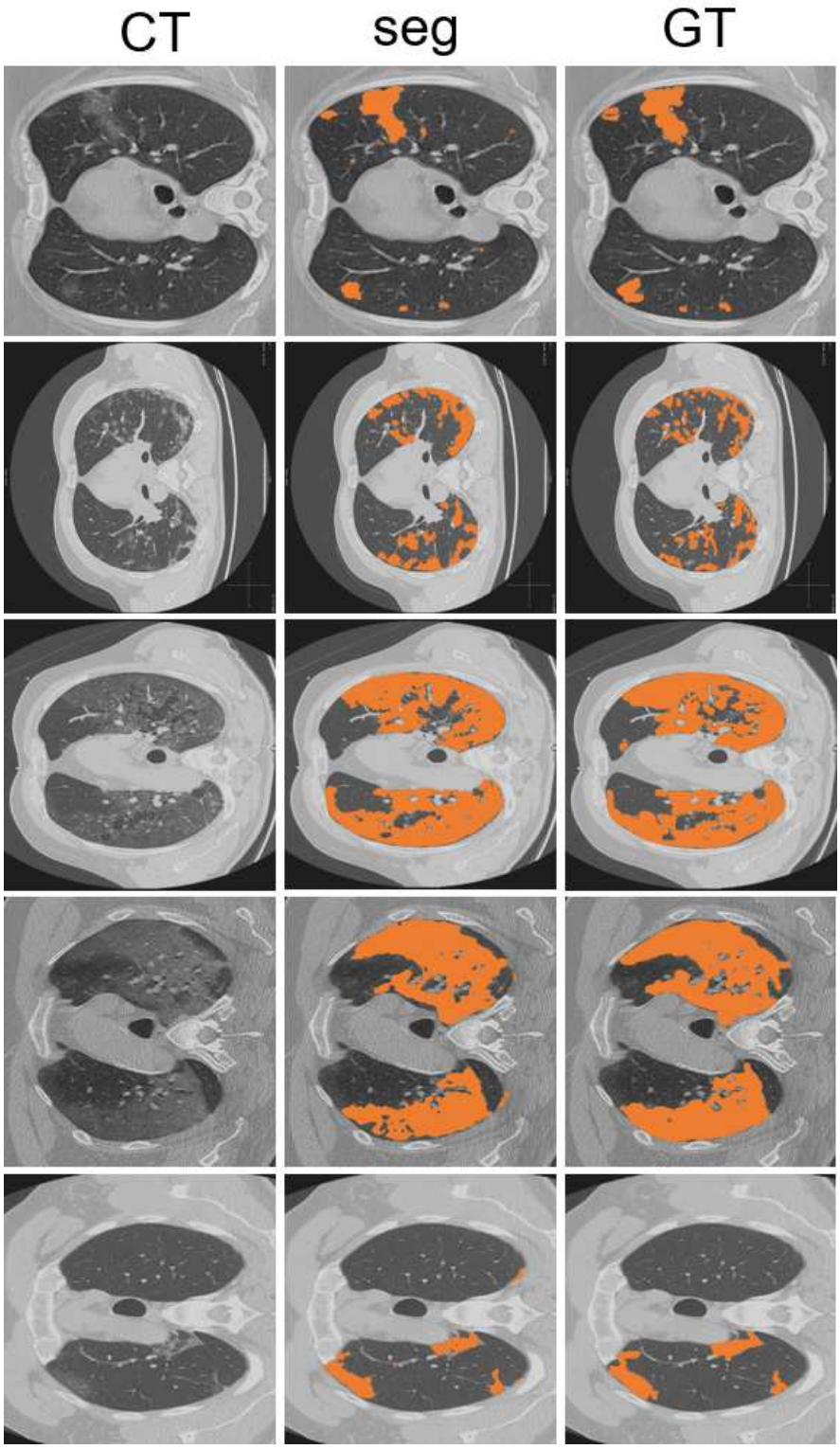

Figure 3

Typical infection segmentation results of CT scans of COVID-19. Columns 1-3: CT image, CT image overlaid with segmentation, and ground truth, respectively.

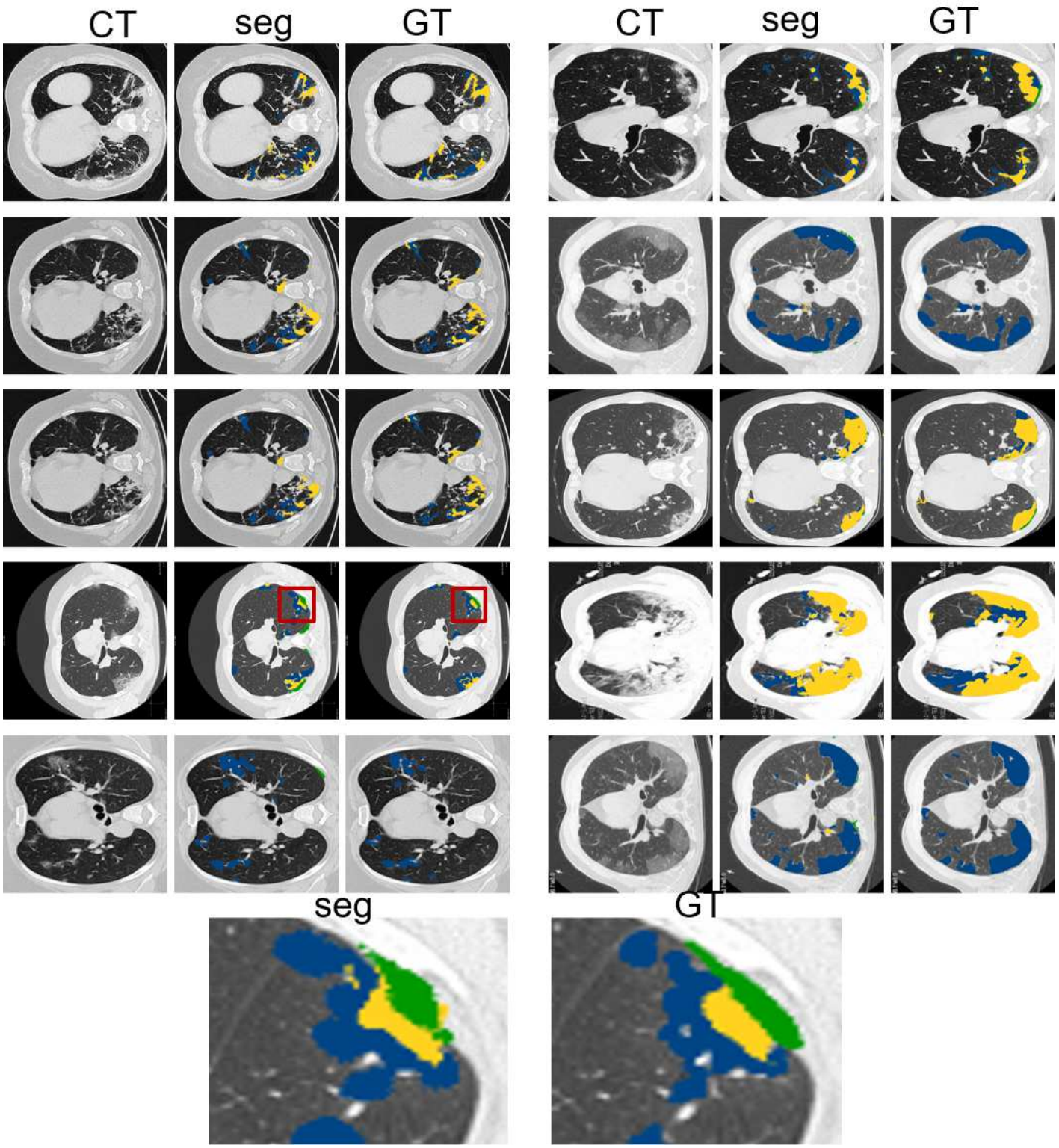

Figure 4

Radiologist-like segmentation results of CT scans of COVID-19. Columns 1-3: CT image, CT image overlaid with segmentation, and ground truth. The blue, yellow, and green labels indicate the ground-glass, consolidation, and pleural effusion, respectively.

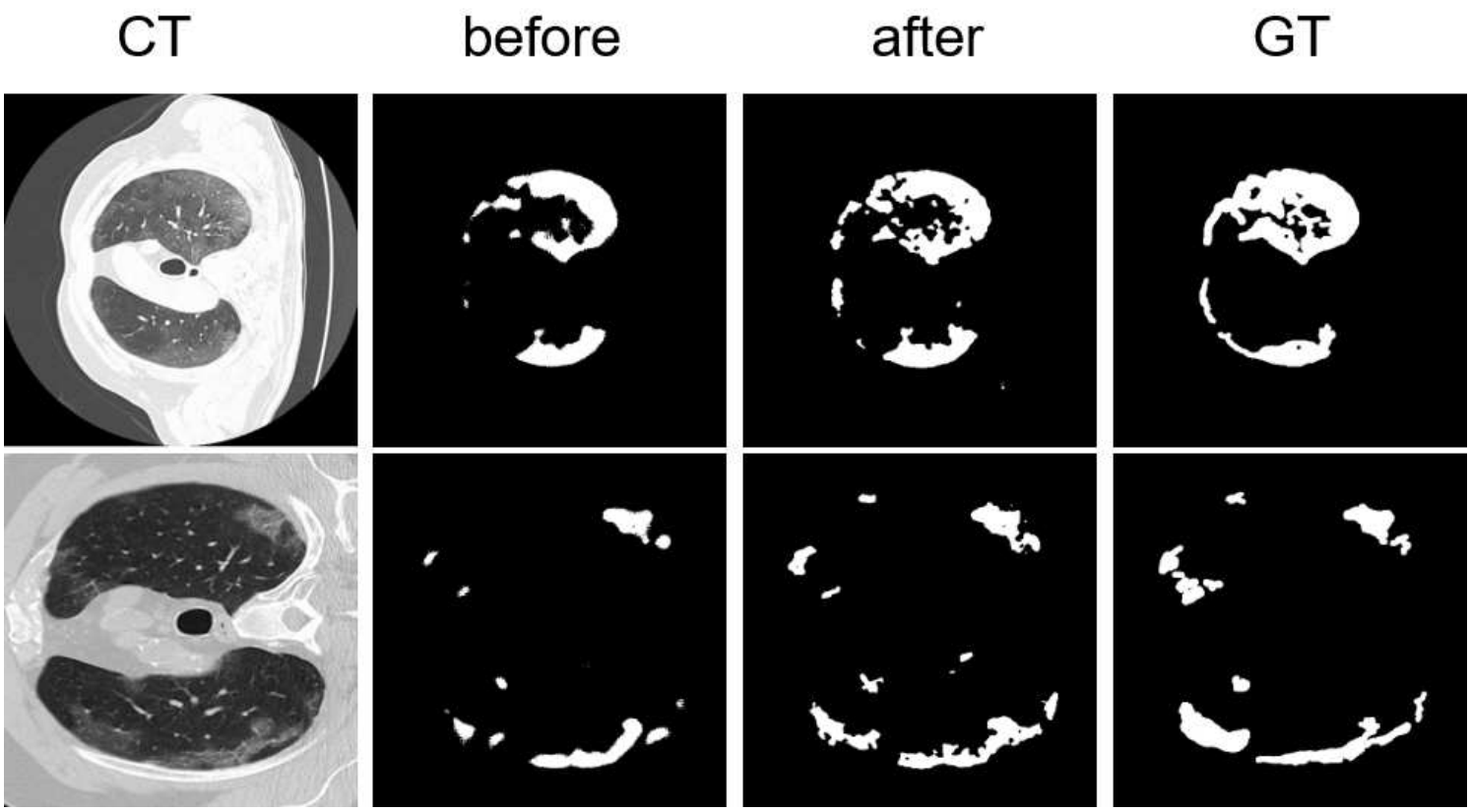

Figure 5

Results comparison of segmentation on CT scans. Columns 1-4: CT images, segmentation results before data distillation, segmentation results after data distillation, and ground truth, respectively.